Electrical Shock Hazard Severity Estimation During Extravehicular Activity for the International Space Station

Douglas R. Hamilton

INTRODUCTION: Research has shown that astronauts performing extravehicular activities may be exposed, under certain conditions, to undesired electrical hazards. This study used computer models to determine whether these undesired induced electrical currents could be responsible for involuntary neuromuscular activity caused by either large diameter peripheral nerve activation or reflex activity from cutaneous afferent stimulation.

METHODS: A multiresolution variant of the admittance method along with a magnetic resonance image millimeter resolution model of a male human body were used to calculate the following: 1) induced electric fields; 2) resistance between contact areas in a Extravehicular Mobility Unit spacesuit; 3) currents induced in the human body; 4) the physiological effects of these electrical exposures; and 5) the risk to the crew during extravehicular activities.

RESULTS: Using typical EMU shock exposure conditions, with a 15V source, the current density magnitudes and total current injected are well above previously reported startle reaction thresholds. This indicates that, under the considered conditions during a spacewalk in the charged ionospheric plasma of space, astronauts could experience possibly harmful involuntary motor response and sensory pain nerve activation.

KEYWORDS: extravehicular activity, extravehicular mobility unit, electrostimulation, International Space Station, nerve action potential, computational simulation, shock hazard, electrical hazard.

Hamilton DR. *Electrical shock hazard severity estimation during extravehicular activity for the International Space Station.* Aerosp Med Hum Perform. 2021; 92(4):231–239.

Astronauts are surrounded by devices which use many different forms of electrical energy to function. Electrical shocks can stimulate physiological responses ranging from a startle reaction, involuntary muscle contraction, seizure, or cardiac arrest. Engineers design hazard controls to prevent humans from being exposed to these electrical hazards in domestic and industrial environments. Electrical hazard risks are mostly controlled by reducing the likelihood of exposure using verifiable fault tolerance. The severity of such exposures is easily understood when voltages and currents reach levels which have been documented to cause deleterious outcomes.[9,10] These effects have been documented by the International Electrotechnical Commission (IEC), which provides basic guidance on the effects of shock current on human beings, livestock and other animals, to derive electrical safety requirements.[9,10]

In many cases these electrical hazards on Earth are controlled and do not result in life threatening outcomes, however, they cannot be proven to be safe for all possible exposures. Regardless, there are some environments where these exposures cannot be controlled, such as during an extravehicular activity (EVA) in low Earth orbit outside the International Space Station (ISS). The Extravehicular Mobility Unit (EMU) that was used for EVAs for the Space Shuttle from 1983 to 2011 was not designed to control for any electrical hazards since those hazards were controlled on the vehicle and all its payloads.

When the ISS was launched, the EMU was recertified to function for those EVAs that involved assembly and repair of the ISS. Unfortunately, the ISS presents a unique electrical

From the Department of Electrical Engineering and Department of Medicine, University of Calgary, Calgary, Alberta, Canada.

This manuscript was received for review in June 2020. It was accepted for publication in February 2021.

Address correspondence to: Douglas R. Hamilton, M.D., Ph.D., M.Sc., General Internal Medicine, University of Calgary, Calgary, Alberta, Canada; Doctorhami@gmail.com.

DOI: https://doi.org/10.3357/AMHP.5702.2021

hazard to the crews during EVAs, that became more significant as the vehicle got larger. Recently, the changes in space weather and more advanced analysis of the ionospheric plasma impedance have allowed NASA to downgrade the hazard to an acceptable level. However, from 2001 until 2012 the ISS program considered all spacewalks to pose an uncontrolled catastrophic electrical hazard to the crew and modeling its likelihood and severity became a top priority.

The ISS Electrical Hazard Description

The Ionosphere composes the Earth's upper atmosphere, between 80 - 600 km, which is bombarded with extreme ultraviolet and X-ray radiation from the Sun. This radiation ionizes neutral oxygen resulting in electrons and oxygen ions being freed to create a 'plasma'. Plasma is the fourth state of matter and behaves electrically different from all other states (air, liquid and solid). Plasma is defined as an electrically neutral yet conductive ionized gas making spacecraft external environments far from being just simple thermal vacuums.[11] The ISS environment is characterized by a wide range of space plasma conditions compounded by ionizing radiation, magnetic fields, micrometeoroids, orbital debris, and other environmental factors, all of which can affect spacecraft or spacesuit performance.[12] Solar radiation varies in an 11-yr cycle causing a commensurate change in the ionosphere's density. The ionosphere is additionally disturbed by other solar phenomena, such as flares, and changes in the solar wind and geomagnetic storms.

The ISS is a large spacecraft with an approximately 100-meter-long main truss moving rapidly through the electrically conducting, magnetized ionospheric plasma and experiences a variable electrical potential in different locations on its structure. Due to the immense physical size and specific characteristics of its photovoltaic electrical power system, the ISS conducting structure can accrue a voltage relative to the surrounding ionospheric plasma. Under certain circumstances, an EVA adjacent to the ISS can expose the astronaut to a risk of electrical shocks ranging from -40 to +160 volts.[2,11,13] The EMU was never designed to operate in this electrically hazardous environment outside the ISS but rather the safe environment inside the Shuttle payload bay. The shock hazard was discovered in 2001 when the ISS robotic arm was to be deployed to assemble the truss. The charge accumulated by the ISS is controlled using plasma couplers which use streams of ionized Xenon gas to pump electrons back into the local ionosphere. This system was originally used to control ISS charge accumulation to protect the anodized surfaces from damage by arcing, however, it was upgraded to be 2-fault tolerant because of the catastrophic shock hazard identified during EVAs. The plasma couplers were made redundant by powering them on independent power buses and controlling them with independent fault detection, isolation and recovery computer systems. Unfortunately, this system occasionally introduced other shock hazards in different parts of the ISS depending on the vehicle attitude with respect to its velocity vector. The complexity of the electrical system of the ISS requires extensive safety analysis for any EVA and sometimes the reason for the EVA is due to an ISS electrical equipment malfunction.

On October 2007, a 2.5-foot tear in one of the ISS solar arrays was discovered during its repositioning and eventual deployment during Shuttle mission STS-120. The arrays had been deployed in earlier phases of the ISS's construction, and the solar panel retraction necessary to move the truss to its new position had not been as smooth as the crew had trained for. During the STS-120 mission, the next EVA was rapidly replanned to allow astronaut Scott Parazynski to ride on the end of the Shuttle's Orbiter Boom Sensor System (OBSS) inspection arm and repair the torn space panels. This EVA was regarded as significantly more dangerous than most because of the possibility of electrical shock (+160 volts) from the solar arrays, the unprecedented and untested use of the OBSS, and the lack of years of EVA planning and training for this impromptu repair. The ISS solar arrays are negatively grounded but have small areas of high voltage (~160 V) positively charged surfaces which are also exposed to the plasma. If parts of the EMU contact the 160 V solar panel, free ionospheric electrons could flow from other EMU metal surfaces and through the astronaut or through the ISS which is negatively grounded. The solar panel repair EVA was successful but there was no doubt about the lethal severity this hazard represented, therefore further shock analysis was not required.

In the typical flight attitude, the ISS truss presents a geometric extension perpendicular to the direction of motion. This motion of the ISS through the Earth's geomagnetic field at both poles induces a voltage, which may distribute on the order of +23 V at both ends of the truss alternating every half orbit as the vehicle crosses the magnetic poles. During the EVAs on STS-120 and STS-123, the crew noticed contamination from metallic shavings and debris in the large drive gear of the starboard Solar Alpha Rotary Joint (SARJ). This joint, together with a similar device on the port side of the station's truss structure, rotates the large solar arrays to keep them facing the Sun. In November 2008, the crew of STS-126 carried out servicing of both the starboard and port SARJs. Analysis showed that the crew could be exposed to the magnetic induction of +23 V volts across the truss at both ends of the SARJ's during the repair EVAs. This lower voltage exposure and its potential current paths through the astronaut required more sophisticated electrical hazard analysis and was the genesis of this study.

This shock hazard is unique to the ISS because of its size and configuration. It is unclear if space vehicles like the ISS will be constructed in the future and the current and future vehicles do not pose a significant risk. As the missions go beyond the Van Allen belt, differential dielectric charging may occur from relativistic charged solar particles; however, this would not pose a threat to an astronaut during a spacewalk.

Extravehicular Mobility Unit

Each segment of the EMU (**Fig. 1**; color versions of figures available online at https://www.ingentaconnect.com/contentone/asma/amhp/2021/00000092/00000004/art00004) is coupled

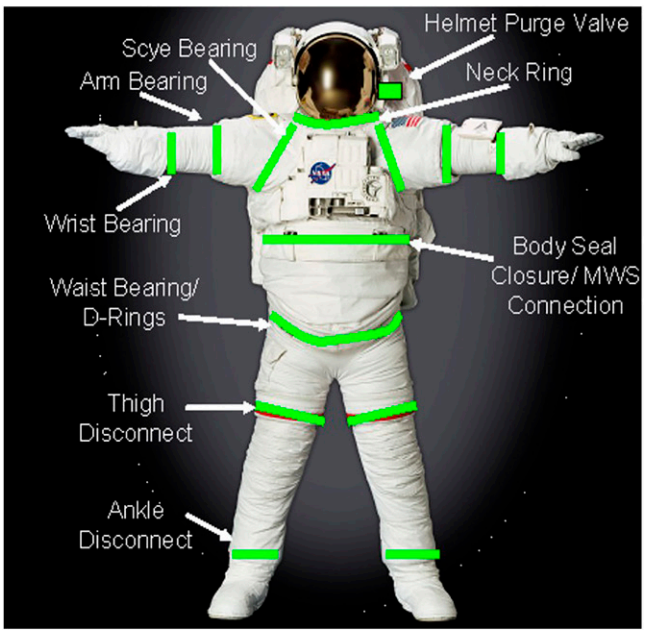

Fig. 1. A. The Extravehicular Mobility Unit (EMU) is composed of several removable components which electrically connect skin with the outside of the suit where the components must be joined by metal rings. **B.** Green bands correspond to places where metal is in contact with both the astronaut's skin and the ionosphere's plasma. [Note: Color version of this figure is available online: https://www.ingentaconnect.com/contentone/asma/amhp/2021/00000092/00000004/art00004.]

together with metallic air-tight bayonet locks. This modular design of the EMU allows it to be easily assembled, disassembled, or modified inside the ISS or Shuttle. The ISS EVA shock hazard was not identified at the time of the vehicle design and therefore the EMU was adopted for ISS EVA operations. In most cases, the outer insulating layer covers the electrical conducting inner layers and components, but exposure of these metallic components to the plasma surrounding the ISS is possible. Furthermore, some exposed metallic components penetrate the suit air retention bladder, providing contact with the sweat-soaked garment on the astronaut's body (Fig. 1, Panel A). During the EVA the astronaut wears a cooling undergarment (Fig. 1, Panel A) connected to a heat exchanger apparatus which radiates heat from the body and equipment into space. Due to the excessive workloads during most EVAs, the astronaut often becomes soaked in perspiration despite the EMU cooling system working at full capacity. The electrically conductive sweat soaked cooling undergarment is in direct contact with the astronaut and metal rings which couple the EMU legs, arms, torso, and helmet sections together (Fig. 1, Panel B).

When the astronaut exits the airlock hatch of the ISS, a steel safety cable is attached from the EMU's waist ring to the ISS. The ISS is surrounded by the Earth's ionosphere, therefore, when astronauts exit the ISS hatch, they become bathed by the conducting plasma. The circuit that enables unwanted electrical shock is formed by the ISS, the steel cable or multiple metallic connecting rings of the EMU, the astronaut and the plasma of the ionosphere (**Fig. 2**). Unfortunately, the current EMU embodiment with multiple metal penetrations permits the conduction of any ISS plasma discharge current through the astronaut via a variety of anatomical pathways (Fig. 1, Panel B). In many cases, the astronaut's body is required to complete the discharge circuit (Fig. 2).

Estimating Electrical Shock Severity

In the past, shock hazard severity has usually been defined by the magnitude of current being conducted through a subject. This was usually determined by estimating the impedance of the path across the body and the exposure voltage. Experiments conducted in the twentieth century on humans and animals determined the physiological response to currents being conducted and their severity (muscle contraction, ventricular fibrillation, burn, etc.).[9] Apart from burns and tissue destruction, most of the physiological response of living systems to electrical shock is due to the E-fields stimulating nerves and/or muscle.[19,20]

Different parts of the human body (e.g., the skin, blood, muscles, other tissues, and joints) present to this EVA shock circuit a cornucopia of impedance pathways composed of resistive and reactive components. The value of total body impedance presented to the circuit depends on a number of factors and, in particular, on current path, touch voltage, duration of current flow, frequency, degree of moisture of the skin, surface area of contact, pressure exerted at the shock interface, and temperature. On Earth the effects of alternating current exposures have been predominantly confined to 50 Hz or 60 Hz which are the most ubiquitous hazards. The human impedance values commonly used for safety design and verification were derived from measurements performed on corpses and, in some cases, living persons.[9] Living subjects have seldom been used due to the uncomfortable sensations and the possibility of lethal hazards involved in electrical exposures using large surface areas of contact (order of magnitude 10,000 mm^2) in dry, water-wet, and saltwater-wet conditions, or with medium (1000 mm^2) and small surface areas of contact (100 mm^2) in dry conditions at touch voltages from 25 to 200 volts.

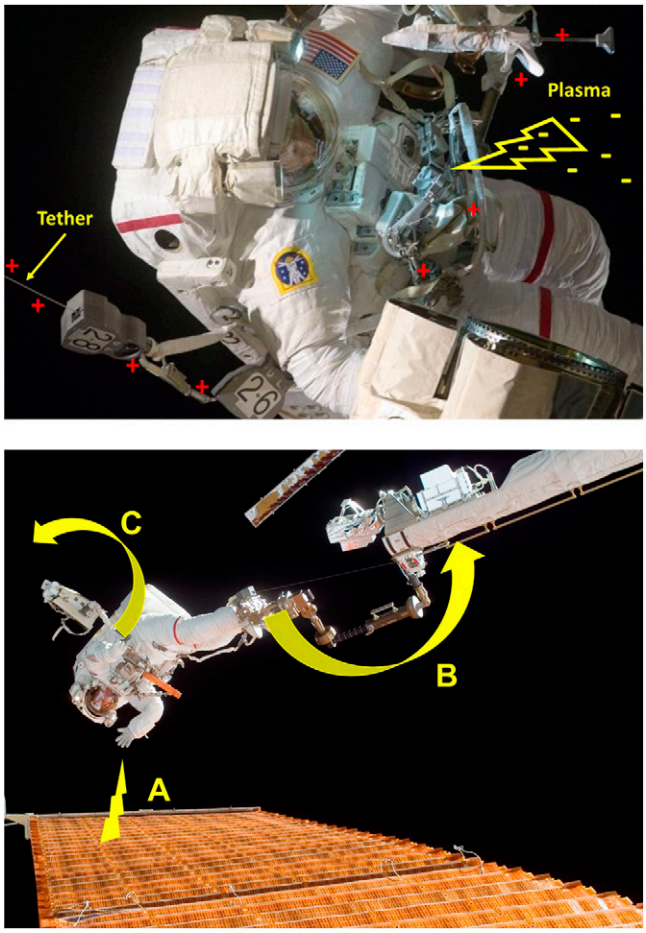

Fig. 2. A. Low voltage positive potential shock circuit where the astronaut is at the end of the SARJ and is 15V positive with respect to the surrounding plasma. The circuit that enables unwanted electrical shock is formed by the ISS, the steel cable connecting the waist ring of the EMU or any other ring which touches the vehicle, the astronaut, or other rings in different locations in the EMU exposed to the ionospheric plasma which supplies free electrons. The free electrons will flow from the plasma into the EMU through metal rings, through the astronaut and onto the ISS from another metal ring in the EMU. **B.** High voltage positive potential shock circuit where the metal ring of the wrist touches the damaged 160-volt solar array (A) and the current then flows through the astronaut and to the ISS which is negatively grounded (B). The current can also flow from the astronaut through a metal ring and into the ionospheric plasma (C). [Note: Color version of this figure is available online: https://www.ingentaconnect.com/contentone/asma/amhp/2021/00000092/00000004/art00004.]

In the case of an EVA, a startle response from an electrical shock could instigate a sudden and involuntary movement from the astronaut causing a lethal hazard or catastrophic damage to a payload. The NASA safety standard[16] requires that if a hazard severity and/or likelihood cannot be adequately quantified then a "worst case" outcome must be assumed and controlled, or waived prior to launch. To estimate the severity of involuntary nerve and muscle activation, the magnitude and rate of change of electric field (E-field) distribution in the body and the E-fields thresholds for nerve or muscle activation need to be considered.

Noxious electrical stimulation is sometimes used to alter the behavior of organisms such as electric fences for ranching. These exposures are designed to produce a startle result in an environment that is safe for the animal or human to react. Conducted Energy Weapons (CEW) or "Tasers" are used to temporarily disable the neuromuscular system by imposing very short but large voltage across the body and thereby exciting neurons in substantial numbers. They are gaining increasing popularity among law enforcement agencies to control violence without permanent damage or fatality to targeted people. Increasing usage of these devices has generated concern regarding the safety of their use on subjects with pre-existing medical conditions.[8,14,25] To address the concern of safety regarding these devices, a number of methods and computational techniques have been used to compute the E-fields and currents in the human body due to exposure to low-frequency electric and magnetic fields.[17]

CEW manufacturers have considered children, pregnant women, the elderly, and very thin individuals to be at higher risk for a serious injury. A study of 25 healthy police volunteers (21 men and 4 women) found no difference in the outcomes between men and women and no significant changes in ventilation, acid-base status, electrolyte concentrations (Ca2+,Na+, K+), troponin I, or ECG's of a clinically relevant nature.[23] The persistence of public controversy surrounding the use of the CEW culminated in October 2007 with a highly publicized incident at the Vancouver International Airport, during which Robert Dziekanski died after being shocked with a taser by Royal Canadian Mounted Police.[3,24] A computer model of the shock hazard from this tragic event was derived by a group of researchers[21] who would eventually be contracted by NASA to become the NASA shock team[15] to perform a similar analysis on the ISS EVA shock hazard.

Because large sensory and motor neurons are significantly more susceptible to electric field activation than direct stimulation of skeletal muscle, the NASA Shock Team[15] chose to consider only nerve excitation to determine the maximum severity of the electrical hazard. Neurons are activated if the E-field or its gradient along the length of the neuron exceeds ion channel activation thresholds which will subsequently propagate further E-field changes along the neuron resulting eventually in neuro-transmitter release to another neuron or an end-effector (muscle, gland, etc.).[18] The E-fields needed to exceed these ion channel activation thresholds are inversely proportional to the diameter of the neurons and the duration of the stimulation.[18]

In order to compute the magnitude and direction of E-fields within the human body, the NASA shock team[15] and NASA Medical Operations[12,13] investigated two different current paths through the astronaut based on analysis of over 100 previous EVAs.[11] The objective of this analysis was to predict anatomical regions in which neurons of different diameters would be excited by electrical shocks consistent with those anticipated during an EVA.

Accordingly, NASA's ISS program contracted several experts to perform the "NASA Extra Vehicular Activity Shock Hazard Research Study"[11,12,15] to model the effects of these electrical hazards on astronauts in an EMU. To understand the effect of

E-field exposure on the human a 3-step process was be performed:

Step 1. Use alternating direction implicit-finite-difference time-domain method to solve for the E-field distribution inside the human body.[15,21]

Step 2. Use the Spatially Extended Nonlinear Node method to predict occurrence of nerve action potentials secondary to the previously calculated E-fields.[19]

Step 3. Establish the physiological reaction to these action potentials such as a startle reaction or involuntary muscle or cardiac activation in the confined EMU.

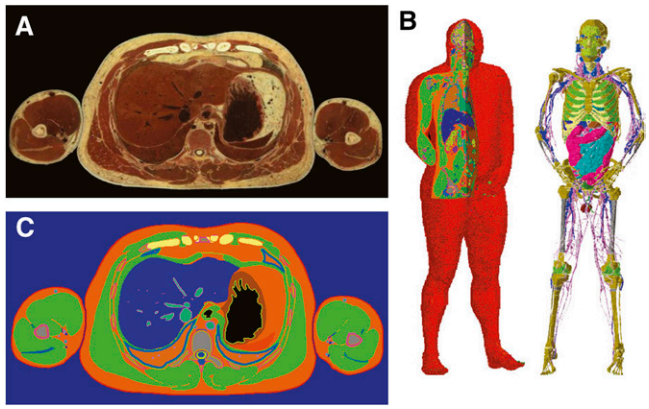

Fig. 3. A. The ADI-FDTD model was applied to an impedance array derived from a total body magnetic resonance image. **B.** This was used to derive the Naval Medical Research Unit San Antonio anatomical man. Each voxel was assigned a conductivity based on tissue type and then included as an element in a network of 335 million lumped impedances. **C.** Because of the very large model size a multiresolution meshing algorithm was used to reduce the number of elements in the model by joining adjacent voxels inside large homogeneous portions of the body, while preserving higher level of detail at anatomical tissue boundaries. (From 'NASA Extra Vehicular Activity (EVA) Shock Hazard Research Study – Phase II.[15]) [Note: Color version of this figure is available online: https://www.ingentaconnect.com/contentone/asma/amhp/2021/00000092/00000004/art00004.]

METHODS

Step 1. Using the ADI-FDTD Model to Estimate E-Field Magnitudes

The Shock team used an Alternating Direction Implicit-Finite-Difference Time-Domain (ADI-FDTD) model to calculate the distribution of E-fields in the body using a multiresolution variant of the admittance method.[15,21] The current paths were determined by the location of electrical contact with metal coupling rings in the EMU, each having 5000 mm^2 area. The first current path was from the sweat-soaked left anterior chest (the EMU body seal closure) to the right waist metal ring where the conductive tether system was attached (Fig. 1, Panel B). A second path was from the left wrist ring to the right waist metal ring (Fig. 1, Panel B). The electrical stimulus waveform used in the computer model was a 4-ms 15-volt, electrical pulse, with a submillisecond rise time. This model is linear and therefore voltages can be scaled from this 15-volt exposure to estimate E-fields from -40 to 160 volts.[15] To address the probability of involuntary nerve excitation, the electric field distribution within major peripheral nerves was determined, as well as current densities and total current injected in the vicinity of the metal contacts.

The ADI-FDTD model was applied to an impedance array derived from a total body magnetic resonance image (**Fig. 3**, Panel A) of the a modified version of the Naval Medical Research Unit San Antonio (NAMRU-SA) anatomical man (Fig. 3, Panel B) which is composed of 586 × 340 × 1878 million 1 mm^3 voxels.[1,22] Tissue conductivities were taken from Gabriel et al.[6,7] at 10 kHz and reported in **Table I**. Each voxel was assigned a conductivity based on tissue type and then included as an element in a network of 335 million lumped impedances.

These impedances are connected to each other using Thevenin circuit theory which results in the calculation of electrical potential at every point (voxel) in the body. Because of the 335 million voxels in the model, the multiresolution meshing algorithm of Cela et al.[4,5] was used to reduce the number of elements in the model by joining adjacent voxels inside large homogeneous portions of the body, while preserving higher level of detail at anatomical tissue boundaries (Fig. 3, panel C).

This model was based on similar analysis performed by Singh et al.[21] which derived the E-field distribution on the human body from a Taser exposure on a subject in Canada. This model was modified to replace the small taser contact areas with two circular cutaneous electrode pads to simulate the contact area of a sweat soaked astronaut and garment to the EMU metal rings.

The contact impedance was modeled based on the extensive human electrical shock measurements for a large surface area and the contact resistance (including skin) was estimated to be 300 Ω per contact.[9] Thus, current circulating through the body meets contact resistance at each of the two electrodes. The internal resistance of the body is calculated using the detailed anatomical model of the human body and the multiresolution impedance method and considering a 1-A current injection between electrodes; under these conditions, the resulting voltage between electrodes is numerically equivalent to the impedance between electrodes. Capacitive effects are considered negligible.[15]

At 1 mm resolution, a radius of 56 voxels was used for each electrode pad to approximate a total contact surface of 5000 mm^2 (**Fig. 4**). The current return electrode was positioned on the right side of the lumbar region where the astronaut touches the metal waist ring.

Two different stimulating electrode placement cases were studied: 1.) from the chest metal ring to waist ring; and 2.) from the left wrist ring to the waist ring.

The skin was removed from the first analysis under the electrodes to obtain perfect contact and then included as a 300-Ω per contact series resistance later in the numerical simulation. The admittance method was used to numerically solve the resulting distribution of E-fields in the Visible Human Male.[1,22]

Table I. Tissue Conductivities at 10 kHz (from Gabriel et al.).[6]

TISSUE	σ [Ω · m]	TISSUE	σ [Ω · m]
Bladder	2.13E-01	Lens	3.35E-01
Blood	7.00E-01	Liver	5.35E-02
Blood Vessel	3.13E-01	Lung Deflated	2.43E-01
Body Fluid	1.50E+00	Lung Inflated	9.32E-02
Bone Cancellous	8.26E-02	Lymph	5.30E-01
Bone Cortical	2.04E-02	Metal	1.00E+04
Bone Marrow	2.74E-03	Mucous Membrane	2.93E-03
Brain Gray Matter	1.15E-01	Muscle	3.41E-01
Brain White Matter	6.95E-02	Nail	2.04E-02
Cartilage	1.76E-01	Nerve	4.24E-02
Cerebellum	1.35E-01	Pancreas	5.30E-01
Cerebro Spinal Fluid	2.00E+00	Retina	5.10E-01
Colon	2.40E-01	Skin Dry (body)	2.04E-04
Cornea	4.43E-01	Small Intestine	5.60E-01
Eye Sclera	5.10E-01	Spleen	1.11E-01
Fat	2.38E-02	Stomach	5.30E-01
Gall Bladder	9.00E-01	Tendon	3.86E-01
Gall Bladder Bile	1.40E+00	Testis	4.30E-01
Gland	5.30E-01	Tooth	2.04E-02
Heart	1.54E-01	Vitreous Humor	1.50E+00
Kidney	1.38E-01		

The ADI-FDTD calculated body impedance was consistent with measured values under condition of wet skin by the IEC[10] decades ago. The peak current injected by a 15-V contact was 18 mA for the chest-to-hip current path (**Fig. 5**) and 15 mA for the wrist-to-hip current path; both of these values are well within the order of the current threshold for startle response.[10] Based on these preliminary results, a conclusion of no electrical hazard during an ISS EVA was not supported by the model.

Step 2. Using the SENN Method to Estimate Sensory and Motor Nerve Activation

Since calculated total body impedances derived from the ADI-FTDT method agrees with the measurements over the last century documented by the IEC,[9] the calculated E-fields inside the subject must now be correlated to the subject's neuromuscular anatomy.[15] To predict occurrence of sensory and motor nerve action potentials secondary to the E-fields from an electrical shock, the well-established Spatially Extended Nonlinear Node (SENN)[19] model of myelinated nerve fiber activation by extracellular E-fields was used by the NASA Shock Team investigators.[15] To estimate the risk of involuntary neuromuscular activation, it was necessary to calculate the E-field strength induced in the body that acts directly on the nerves (Fig. 5).

The magnitude of the E-field needed to stimulate a peripheral nerve when the field is not parallel to the nerve fiber and applied to the distal ends of the fiber was 6.15 V/m for axons of ≈20 μm diameter (**Table II**).[15,20] The threshold, or minimal stimulus, required to stimulate neuronal tissue is inversely proportional to the nerve diameter and was exceeded in most of the neural tissue in the left arm for the hip-to-wrist shock path scenario.[15,20]

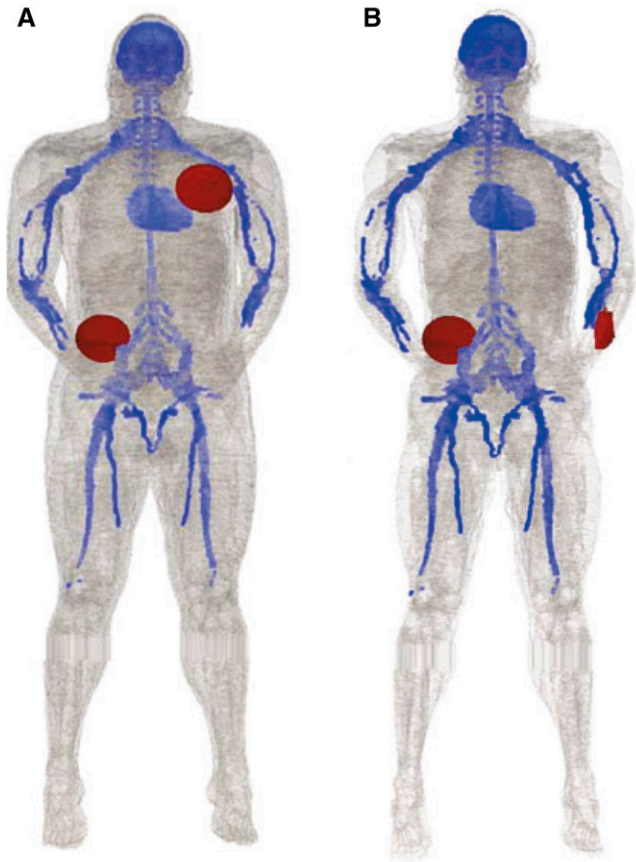

Fig. 4. The NAMRU anatomical model with the location of the major peripheral nerves shown in dark gray (color blue online). Electrode geometry and placement (black circle; color red online) is shown for: **A.** Chest to Hip exposure; and **B**. Wrist to Hip exposure. (From 'NASA Extra Vehicular Activity (EVA) Shock Hazard Research Study – Phase II.[15]) [Note: Color version of this figure is available online: https://www.ingentaconnect.com/contentone/asma/amhp/2021/00000092/00000004/art00004.]

The advantages of this modeling method are illustrated in Fig. 5 where the current densities vary with anatomy. Fig. 5 shows a transverse slice through the center of the chest electrode in the chest-to-hip shock configuration. Current density distribution in the proximity of the chest electrode illustrates current-preferred current path around high impedance of the inflated lung.

RESULTS

Posture, locomotion, and sensory stimulus response are primarily controlled by the central nervous system. The spinal cord controls the patterns of spinal neuron action potential pulses which translate into coordinated motor responses so that flexor and extensor muscles are always in balance. An external nonphysiological excitation of a motor neuron by an electrical shock might cause a nonpurposeful and possibly harmful muscle response. Furthermore, the stimulation of sensory neurons by external nonphysiological signals could also trigger reflex movements mediated by the spinal cord and/or brain. In both situations, stimulation of a peripheral nerve by an electrical

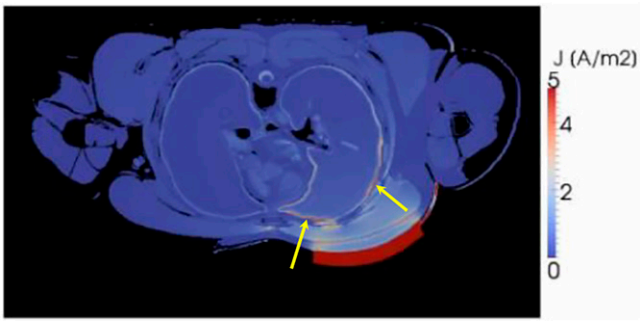

Fig. 5. Chest-to-hip current density at the transverse slice through center of the anterior chest electrode. Current density distribution in the proximity of the chest electrode illustrates current-preferred current path (white arrows; yellow online) around the high impedance inflated lung. [From 'NASA Extra Vehicular Activity (EVA) Shock Hazard Research Study – Phase II.[15]] [Note: Color version of this figure is available online: https://www.ingentaconnect.com/contentone/asma/amhp/2021/00000092/00000004/art00004.]

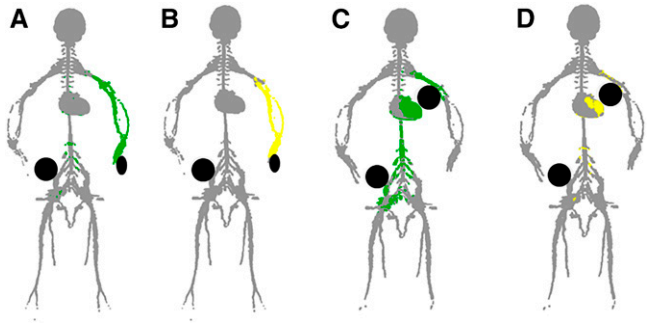

Fig. 6. Frontal view of predicted nerve activation for 10-20 μm diameter peripheral nerves (dark grey; green online) and 5-10 μm diameter peripheral nerves (light grey; yellow online). These are shown for a left wrist to right hip exposure (Panels A and B) and left anterior chest to right hip exposure (Panels C and D). The black circles represent where the electrodes made body contact. (From 'NASA Extra Vehicular Activity (EVA) Shock Hazard Research Study – Phase II.[15]) [Note: Color version of this figure is available online: https://www.ingentaconnect.com/contentone/asma/amhp/2021/00000092/00000004/art00004.]

shock could result in an astronaut's injury and/or damage to equipment.

Different diameter nerves have different physiological functions and therefore the response to exciting these different nerve types would differ. This is important when predicting the body response to an EVA shock. **Fig. 6** (See color version online at: https://www.ingentaconnect.com/contentone/asma/amhp/2021/00000092/00000004/art00004) reveals that a 15-V electrical shock between the wrist and the waist is likely to excite Type I and Type II peripheral nerve fibers along major nerve tracts in the extremity through which the current passes. This would cause a possible startle response and/or involuntary and simultaneous flex and extensor muscle activation.[15] Therefore a 15-V electrical shock to the left wrist is likely to cause involuntary movement of the left upper extremity mediated by either direct motor nerve stimulation in the median, ulnar, or radial nerves. In addition, a generalized involuntary motor response in the entire body could be triggered by direct stimulation of left upper extremity sensory nerves which may trigger a spinal reflex. In the case of the chest to waist exposure, only the largest diameter Type I myelinated fibers would be excited (Fig. 6).

A strong neuromuscular response resulting from direct stimulation of a major nerve trunk is unlikely for a 15-V electrical shock if the electrode path is from the waist to anterior chest. However, if one electrode was immediately adjacent to the brachial plexus, a more likely outcome would be an involuntary startle reaction mediated by spinal reflexes or simultaneous stimulation of flexor and extensor motor nerves with possible muscle trauma.[15]

Table II. Action Potential Threshold Criteria for Nerve Stimulation When the E-Field Is Parallel to the Nerve Fiber.*

FIBER DIAMETER (μm)	THRESHOLD E-FIELD (V/m)
20	6.15
10	12.3
5	24.3
2.5	49.2

* For largest diameter mammalian nerves, a field threshold of approximately 6.15 (volts/meter) of at least 2 milliseconds is required for excitation of an action potential.

DISCUSSION

The E-fields measured from a 15-V source across the body at specific contact points in the EMU resulted in nerve activation with its physiologically harmful sequalae. This demonstrates that even low voltages can be harmful under certain circumstances. If the E-fields in those regions exceed the perception threshold by a sufficient factor, subjects can experience a reflex reaction. This is confirmed by the fact that the magnitude of current induced by the 15-V shocks is well in excess of the 2-mA current magnitudes required to produce a startle response in humans according to the IEC.[9] This startle response is primarily mediated by stimulation of sensory nerves. Thus, the NASA Shock Team concluded that the risk of involuntary motor response is predicted to be substantial with a 15-V electric shock under the assumptions of the model.[15]

Further investigation is needed to verify this model. In the limited exposure scenarios in this study a conservative contact resistance of 300 Ω per contact point was used (**Fig. 7**). If the skin was soaked with perspiration, the contact resistance could be closer to subepidermal tissue which was modeled as no contact resistance. (Most cardiac defibrillators are calibrated assuming a 25-Ω transthoracic impedance.) These results suggest the EVA shock prime mover resembles a voltage source and the added 600 Ω series resistance of intact moist skin reduced field strength in the body by roughly 50% (Fig. 7). This study could not confirm, nor rule out, a cardiac shock hazard with a chest to waist exposure.

To determine the shock hazard severity in any industrial environment, several sequential tasks need to be performed. **Fig. 8** itemizes the steps needed to determine the shock hazard severity for an EVA on the ISS using the additional modeling tools described in this study. To properly verify this model, we

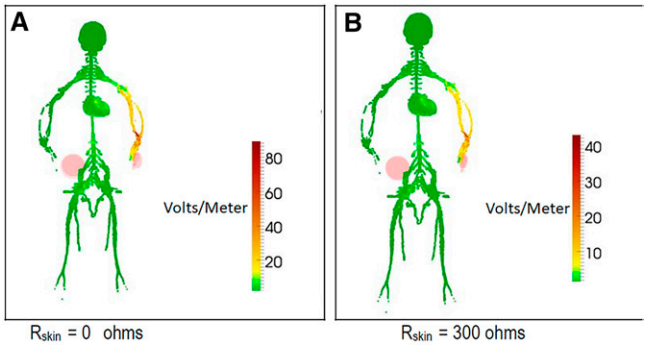

Fig. 7. Frontal view of E-field magnitude distribution along nerves, heart, and spinal cord when electrode contacts are left wrist and right waist for conditions of no skin resistance [0Ω panel (**A, left**)] and saturated wet skin [300Ω panel (**B, right**)]. Major peripheral nerves, central nerves and heart color coded according to the induced electric field magnitude. The contact electrodes (shown as light gray circles; pink online) are located on the anterior chest and right hip. The E-field scaling between panels has changed; nonetheless the presence of skin reduces the E-fields in the body by 50%. (From 'NASA Extra Vehicular Activity (EVA) Shock Hazard Research Study – Phase II.[15]) [Note: Color version of this figure is available online: https://www.ingentaconnect.com/contentone/asma/amhp/2021/00000092/00000004/art00004.]

would need further study involving models and possible animal and human studies with safe continuous and toggled direct current waveforms. Human experiments are needed to confidently define the skin impedance model for the exposure conditions expected in the ISS for inputs to the multiresolution admittance method model. Solving for the E-field magnitudes in the skin under the metal-skin interface would allow for more accurate prediction of cutaneous sensory response and withdrawal reflexes.

Although this shock hazard has been remediated due to changes in space weather and a better understanding of the conducting plasma, this modeling method can be used for other shock exposures. This new electrical hazard analysis technique shows promise in helping control low voltage electrical hazards in areas such as aerospace, automotive, gaming, and toy industries.

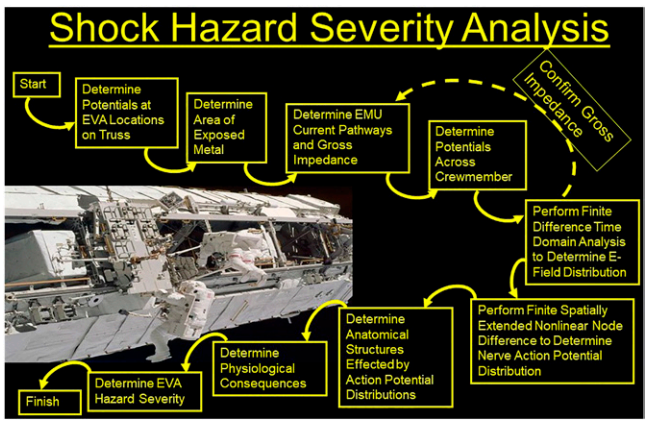

Fig. 8. Steps needed to determine the shock hazard severity for an EVA on the ISS using the additional modeling tools described in this study.

ACKNOWLEDGMENTS

The operational impact and physiological sequalae of the shocks during an EVA were performed by the Extravehicular Activity Integrated Project Team at the NASA Johnson Space Center based on a study funded by NASA for the Electrokinetic Signal Research Incorporated to perform the Spatially Extended Nonlinear Node and Alternating Direction Implicit-Finite-Difference Time-Domain analysis of the International Space Station Solar Alpha Rotary Joint extravehicular activity electrical shock hazard. (Army contract number W911QY-08-D-0024).

Financial Disclosure Statement: The author has no competing interests to disclose.

Author and affiliation: Douglas R. Hamilton, M.D., Ph.D., M.Sc., Department of Electrical Engineering and Division of General Internal Medicine, University of Calgary, Calgary, Alberta, Canada.

REFERENCES

1. Ackerman MJ, Spitzer VM, Scherzinger AL, Whitlock DG. The visible human data set: an image resource for anatomical visualization. Medinfo. 1995; 8(Pt. 2):1195–1198.
2. Barsamian H, Mikatarian RR, Minow JI, Alred J, Koontz S. editors. ISS plasma interaction: measurements and modeling. 8th Spacecraft Charging Technology Conference; Oct. 20–24, 2003; Marshall Space Flight Center, Huntsville, AL. Huntsville, AL: NASA; 2003. NASA/CP-2004-213091.
3. Canadian-Broadcasting-Corporation. Controversy over RCMP use of Taser on Sussex. 2008. [Accessed June 2020.] Available from: https://www.cbc.ca/news2/background/tasers/video.html.
4. Cela CJ. A Multiresolution Admittance Method for Large-scale Bioelectromagnetic Interactions. North Carolina State University; 2010:103.
5. Cela CJ, Lee RC, Lazzi G. Modeling cellular lysis in skeletal muscle due to electric shock. IEEE Trans Biomed Eng. 2011; 58(5):1286–1293.
6. Gabriel S, Lau RW, Gabriel C. The dielectric properties of biological tissues: II. Measurements in the frequency range 10 Hz to 20 GHz. Phys Med Biol. 1996; 41(11):2251–2269.
7. Gabriel S, Lau RW, Gabriel C. The dielectric properties of biological tissues: III. Parametric models for the dielectric spectrum of tissues. Phys Med Biol. 1996; 41(11):2271–2293.
8. Holden SJ, Sheridan RD, Coffey TJ, Scaramuzza RA, Diamantopoulos P. Electromagnetic modelling of current flow in the heart from TASER devices and the risk of cardiac dysrhythmias. Phys Med Biol. 207; 52(24):7193–7209.
9. International Electrotechnical Commission. Effects of current on human beings and livestock. Part 1 (TS 60479). 4th ed. Geneva, Switzerland: International Electrotechnical Commission; 2005–2007.
10. International Electrotechnical Commission. Use of conventional touch voltage limits. Part 5 (TR 61201). 4th ed. Geneva, Switzerland: International Electrotechnical Commission; 2006.
11. Koontz S, Castillo T, Hartman W, Schmidl W, Haught M, et al. International Space Station spacecraft charging hazards: Hazard identification, management, and control methodologies, with possible applications to human spaceflight beyond LEO. Proceedings of the 10th IAASS Conference, May 15–17, 2019, El Segundo, CA, USA. Noordwijk, The Netherlands: ESA Communications ESTEC, 2019.
12. Kramer L, Hamilton D, Mikatarian R, Thomas J, Koontz S. editors. Positive voltage hazard to EMU crewman from currents through plasma. Proceeding of the 4th IAASS Conference, 'Making Safety Matter'; May 19–20, 2010; Huntsville, Alabama, USA. Noordwijk, The Netherlands: ESA Communications ESTEC, 2010.
13. Kramer L, Hamilton DR. EVA electroshock hazard from currents through plasma. In: Kanki BG, Clervoy J, Sandal G, Sgobba T, editors. Humans Systems Interface Design. 1st ed. Oxford (UK): Butterworth-Heinemann; 2017:56–63.

14. Kunz SN, Calkins H, Adamec J, Kroll MW. Cardiac and skeletal muscle effects of electrical weapons. Forensic Sci Med Pathol. 2018; 14(3):358–366.
15. Lee R, Lazzi G, Reilly P, Ziriax J. NASA Extra Vehicular Activity (EVA) Shock Hazard Research Study – Phase II. Chicago, IL: Electrokinetic Signal Research, Inc; 2011. Army contract no. W911QY-08-D-0024.
16. NASA. Crew Health. Space Flight Human-System Standard, Vol. 1. Houston (TX): NASA Johnson Space Center; 2015; NASA-STD-3001.
17. Panescu D. Fau - Kroll MW, Kroll MW, Efimov IR, Sweeney JD, Panescu D. Finite element modeling of electric field effects of TASER devices on nerve and muscle. Conf Proc IEEE Eng Med Biol Soc. 2006; 2006:1277–1279.
18. Patrick Reilly J, Diamant AM, Comeaux J. Dosimetry considerations for electrical stun devices. Phys Med Biol. 2009; 54(5):1319–1335.
19. Reilly JP. Applied applied bioelectricity—from electrical stimulation to electropathology. New York (New York): Springer-Verlag; 1998.
20. Reilly JP, Diamant AM. Spatial relationships in electrostimulation: application to electromagnetic field standards. IEEE Trans Biomed Eng. 2003; 50(6):783–785.
21. Singh V, Ajeet A, Kwatra N, Cela CJ, Ziriax J, et al. Computation of induced current densities in the human body at low frequencies due to contact electrodes using the ADI-FDTD method. IEEE Transactions on Electromagnetic Compatibility. 2010; 52(3):537–544.
22. Spitzer V, Ackerman MJ, Scherzinger AL, Whitlock D. The visible human male: a technical report. J Am Med Inform Assoc. 1996; 3(2):118–130.
23. Vilke GM, Sloane CM, Suffecool A, Kolkhorst FW, Neuman TS, et al. Physiologic effects of the TASER after exercise. Acad Emerg Med. 2009; 16(8):704–710.
24. Zaychenko VA, Verdun-Jones SM. Police use of conducted energy weapons: a review of the Canadian jurisprudence. Vancouver, Canada: Simon Fraser University; 2011.
25. Zipes DP. Sudden cardiac arrest and death following application of shocks from a TASER electronic control device. Circulation. 2012; 125(20):2417–2422.